Effects of distance-dependent delay on small-world neuronal networks

Jinjie Zhu,* Zhen Chen, and Xianbin Liu†
State Key Laboratory of Mechanics and Control of Mechanical Structures, College of Aerospace Engineering, Nanjing University of Aeronautics and Astronautics, Nanjing 210016, China
(Received 23 November 2015; revised manuscript received 28 January 2016; published 28 April 2016)

We study firing behaviors and the transitions among them in small-world noisy neuronal networks with electrical synapses and information transmission delay. Each neuron is modeled by a two-dimensional Rulkov map neuron. The distance between neurons, which is a main source of the time delay, is taken into consideration. Through spatiotemporal patterns and interspike intervals as well as the interburst intervals, the collective behaviors are revealed. It is found that the networks switch from resting state into intermittent firing state under Gaussian noise excitation. Initially, noise-induced firing behaviors are disturbed by small time delays. Periodic firing behaviors with irregular zigzag patterns emerge with an increase of the delay and become progressively regular after a critical value is exceeded. More interestingly, in accordance with regular patterns, the spiking frequency doubles compared with the former stage for the spiking neuronal network. A growth of frequency persists for a larger delay and a transition to antiphase synchronization is observed. Furthermore, it is proved that these transitions are generic also for the bursting neuronal network and the FitzHugh-Nagumo neuronal network. We show these transitions due to the increase of time delay are robust to the noise strength, coupling strength, network size, and rewiring probability.

DOI: 10.1103/PhysRevE.93.042417

I. INTRODUCTION

Since the work from Watts and Strogatz in 1998 [1], small-world (SW) networks have attracted great attention from many disciplines since the SW property seems to be a quantifiable (and intuitive) characteristic of many real-world structures, both human, generated (social networks, World Wide Web, power grid), or of biological origin (neural and biochemical networks) [2]. Especially in neuroscience, researchers have devoted a lot to the dynamical behaviors and biological mechanisms of the neurons in SW networks [3–6]. Humphries *et al.* [3] demonstrated that the brainstem reticular formation was a small-world network, not scale free. A two-dimensional square lattice model was employed by Perc [4] to investigate the effects of small-world connectivity on noise-induced temporal and spatial order. Bassett and Bullmore [5] gave a review about how the concept of small-world networks and corresponding methods could be used to study our complex brain so as to better understand the structure and function of human brain systems. Lago-Fernández *et al.* [6] investigated the role that different connectivity regimes play in the dynamics of a network of Hodgkin-Huxley neurons. They found that SW topologies took advantage of the best features of both random and regular ones, giving rise to fast system response with coherent oscillations. More recently, Zheng *et al.* [7] studied the spatiotemporal patterns and firing synchronization with noise and small-world connectivity. It was found that there existed an optimal fraction of randomly rewired links that maximized the temporal order and synchronization.

Neuron models have sprung up after the work of Hodgkin and Huxley [8]. Classical models, including the FitzHugh-Nagumo (FHN) model [9], the Hindmarsh-Rose (HR) model [10], and the Morris-Lecar (ML) model [11], are mostly described by differential equations. A two-dimensional map model which contained one fast and one slow variable, was introduced by Rulkov to replicate the dynamics of spiking and spiking-bursting activity of real biological neurons [12,13]. Due to its efficiency in capturing all the main dynamical features and its simplicity in computation, the Rulkov model has engaged much attention [14–17]. Batista *et al.* [14] investigated the chaotic phase synchronization in a scale-free network with the Rulkov model. Ivanchenko *et al.* [15] studied chaotic phase synchronization of the Rulkov model with mean field coupling. They showed the transition to mutual synchronization by introducing an order parameter and found the external synchronization by adding a harmonic signal to one arbitrary neuron. Wang and his team [16,17] made efforts in the square lattice neuronal network to study on the collective behavior, benefiting from the convenient computation of the Rulkov model, and they found abundant collective dynamical behaviors such as pattern formations, and different kinds of synchronizations, resonance, etc.

Time delay is inevitable in the nervous system due to the finite speed of signal transmission over a distance and the time lapses occurring by both dendritic and synaptic processes [18]. It is proved that the speed of signal conduction through unmyelinated axonal fibers is on the order of 1 m/s resulting in time delays up to 80 ms for propagation through the cortical network [19]. Time delay can cause nontrivial phenomena in neuronal networks, such as periodicity [20], synchronization [19], resonance [21], phase transition [22], fruitful spatiotemporal patterns [23,24], etc. Recently, distributed delay has become a new direction to investigate the complex behaviors in neuronal networks [25–27]. However, the spatial distance between neurons, which is a main source of delay naturally from the relation of time to distance, has seldom been taken into investigation. Distance-dependent delays have been studied in oscillators on square lattice networks [28–30] and ring coupled networks [31]. For square lattice networks, some researchers considered delay to be related to the distance along

*jinjiezhu@nuaa.edu.cn
†xbliu@nuaa.edu.cn

the lattice [29], while others considered delay to be linearly related to the two-dimensional (2D) Euclid distance between oscillators [28,30]. Specifically, a review on various types of delays (e.g., constant, distributed, and distance-dependent delays) examined the role of delays on coupled systems of neuronal oscillators [32]. Yet, the effects of the distance between neurons on the firing behaviors and corresponding spatiotemporal patterns with other network topologies are not clearly understood, and thus deserve deeper research.

Consequently, the main purpose of this paper is to explore the effects of the distance between neurons in small-world networks, as well as the robustness of these effects to the other parameters, e.g., network size, rewiring probability, noise strength, and coupling strength. This paper is organized as follows. First, the theoretical model is introduced and the corresponding parameters are initially set. Second, the main results are obtained by using numerical methods. Finally, some conclusions and discussions are given.

II. MATHEMATICAL MODEL AND SETUP

The model used here is the Rulkov map [12]. We consider the small-world coupling, with Gaussian noise and time delay. In contrast to the work of Wang [18], delay in our work is related to the distance between neurons. Thus, the dynamical behavior is governed by the following equations:

$$x^i(n+1) = \frac{\alpha}{[1+x^i(n)^2]} + y^i(n) + w\xi^i(n) + D\sum_{j=1\ldots N}\varepsilon_{ij}[x^j(n-\tau_{ij}) - x^i(n)], \quad (1)$$

$$y^i(n+1) = y^i(n) - \sigma x^i(n) - \beta, \quad i = 1\cdots N,$$

where $x^i(n)$ and $y^i(n)$ are, respectively, the fast and slow dynamical variables of the ith neuron; w is the intensity of the noise, with $\xi^i(n)$ being independent, zero mean, Gaussian noise which is characterized by $\langle\xi^i(n)\rangle = 0$ and $\langle\xi^i(n)\xi^j(m)\rangle = \delta_{ij}\delta_{nm}$, where $\delta_{xy} = 1$ if $x = y$, and $\delta_{xy} = 0$ otherwise. D is the coupling strength of the gap junctions, and ε_{ij} measures the connectivity between the ith and jth neuron, whereby $\varepsilon_{ij} = 1$ and 0 indicate the ith is connected with the jth neuron or not, respectively. σ,β reflect the slow evolution of $y^i(n)$, and with different values of α, a single neuron will produce complex dynamical properties. In this system, for $\alpha < 2$, the neuron will stay quiescent without the aid from noise, while for $\alpha > 2$, the neuron will exhibit behaviors such as periodic spiking, bursting, chaotic spiking-bursting, etc. For the time being, we set $\alpha = 1.95$, $\sigma = \beta = 0.001$ throughout this paper as the neuron is noise excitable.

τ_{ij} is the information transmission time delay between neurons i and j (the number is sorted counterclockwise), which is the main parameter discussed in this paper. A typical small-world network is shown in Fig. 1(a) generated by the method mentioned in Ref. [1]. At present, we set $N = 150$ vertices, with $k = 4$ nearest neighbors coupled and rewiring probability $p = 0.1$. The time delay is $\tau_{ij} = \tau_e d_{ij}$, where d_{ij} is the distance between neurons i and j, and τ_e is the element time delay related to the information transmission speed. As such, the time delay in the same network between different neurons will be totally different. The farther the distance, the longer the delay will be [see Fig. 1(b)]. In this study, we set the delay related to the 2D Euclid distance between neurons. For example, the delay between neurons i and j is as follows:

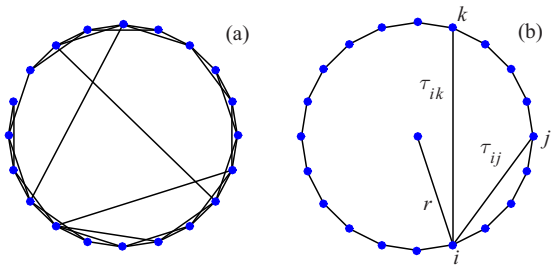

FIG. 1. Typical connection of a small-world network and the explanation for the time delay related to distance. (a) A ring structured small-world network is displayed with vertices $N = 20$ and connections to $k = 4$ nearest neighbors, and the rewiring probability $p = 0.2$. (b) The explanation of the time delay related to distance between neurons in the network. From the figure, the distance between neurons i and k is larger than that of neurons i and j, as a consequence, the time delay from neuron i to k is larger than the latter.

$$\tau_{ij} = \mathrm{int}(\tau_e d_{ij}) = \mathrm{int}\left\{\tau_e\left[2r\sin\left(\frac{\pi\times\mathrm{dist}}{N}\right)\right]\right\}, \quad (2)$$

where $\mathrm{dist} = \min(N-|i-j|,|i-j|)$, and $\mathrm{int}(\cdot)$ calculates the nearest integer of the quantity inside the brackets due to the discrete map.

Noise is also inherent in the neuronal activities [33]. Because $\alpha = 1.95 < 2$, without the aid from the noise, the neurons will stay in quiescence. So independent Gaussian noise is added to excite the neurons. Noise should neither be set so weak that the neurons will not fire so frequently, nor too strong in that strong enough noise will drown the main features of the dynamical behaviors. Thus, by experimenting with different strengths of noise, $w = 0.01$ was selected to assist our research [see Fig. 2(a)].

III. RESULTS

In this section, spatiotemporal patterns and interspike intervals (ISIs) as well as the interburst intervals (IBIs) will be

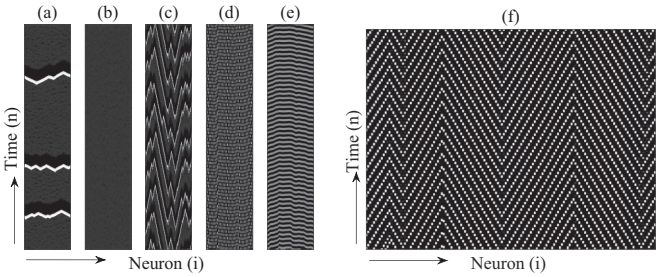

FIG. 2. Spatiotemporal pattern plots of $x^i(n)$ obtained for different time delays. From (a) to (e), the element time delay τ_e equals 0, 700, 1500, 3400, and 4500 (for convenience, we set $r = 1$). (f) is the enlargement of (d), which shows the regular zigzag pattern. The color is linearly divided into ten levels with white depicting 0.0 and black depicting –1.5 values. Other parameters are $N = 150$, $w = 0.01$, $p = 0.1$, and $D = 0.02$.

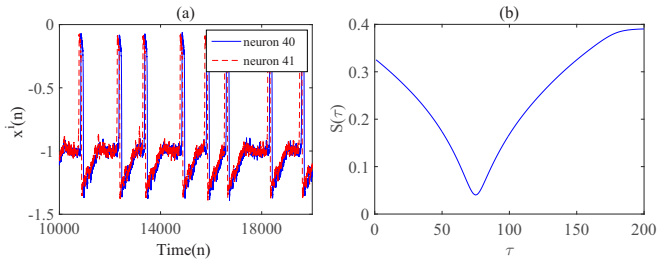

FIG. 3. Time series for neurons 40 and 41 and the corresponding similarity function [parameters are the same as in Fig. 2(c)]. (a) The time series for neurons 40 and 41 are characterized by solid blue line and dashed red line, respectively. They are qualitatively the same except for a phase lag. (b) From the similarity function, the minimum is obtained at a time shift of 75, where $S(\tau)$ is less than 0.05, that shows a lag synchronization between the two neurons.

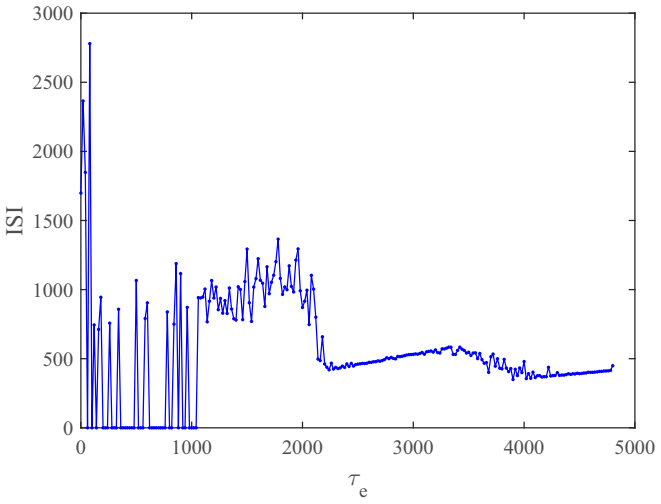

FIG. 4. The interspike intervals (ISIs) of $x^i(n)$ on different element time delays. The ISIs for different delays were obtained by averaging over time (1×10^4 iteration steps) and space (all neurons) (computations for ISIs and IBIs below are done in the same way). There were roughly four stages to be seen within the delay range in the figure: 0–1100, 1100–2100, 2200–3500, and 4100–4800. The first stage: delay intermittently disturbed the firing behaviors; the second stage: delay-induced irregular zigzag patterns; the third stage: delay-induced regular zigzag patterns; finally, delay-induced antiphase synchronizations. Parameters are the same as in Fig. 2.

used to investigate the collective behaviors and the transitions among them in our system (all spatiotemporal patterns, ISIs, and IBIs are plotted about the fast variable throughout this paper). At first, parameters are fixed except the time delay to study the spatiotemporal behaviors in small-world networks. Five classical patterns are illustrated in Fig. 2 with different time delays. In the absence of time delay, we can see from Fig. 2(a) that the neurons can fire intermittently but almost simultaneously. This is a noise-induced firing phenomenon which is beyond the scope of this paper. As the time delay is taken into consideration, firing behaviors can be disturbed by relatively small time delays. There is no spike in Fig. 2(b) demonstrating that all neurons are quiescent. This means that small time delays can disturb or even destroy the collective firing behaviors. By increasing the time delay, irregular zigzag patterns will emerge as is illustrated in Fig. 2(c). This is a delay-induced phenomenon which differs from Fig. 2(a). The neurons fire periodically with a phase lag [see Fig. 3(a)] and this is actually the so-called lag synchronization [34] which was reflected by the similarity function defined as $S^2(\tau) = \langle [x_2(t+\tau) - x_1(t)]^2 \rangle / [\langle x_1^2(t) \rangle \langle x_2^2(t) \rangle]^{1/2}$ (τ is the time shift, please do not confuse with the time delay in this paper). When the similarity function $S(\tau)$ reaches its minimum 0 for $\tau = 0$, it means complete synchronization. When $S(\tau)$ reaches its minimum for nonzero time shift τ, it means a time lag exists between two processes. By using the similarity function, the phase lag can be quantitatively calculated as in Fig. 3(b) ($\tau_e = 1500$). By further increasing the delay, a phenomenon will arise which exhibits regular zigzag patterns [see Fig. 2(d) and the enlargement, Fig. 2(f)]. More interestingly, the firing frequency had a sudden increase which we will calculate quantitatively later. Finally, the frequency-increasing effect is found again for a larger delay, and the firing behavior transits from regular zigzag pattern to antiphase synchronization.

For a more detailed and accurate analysis, we calculate the interspike intervals. As we can see from Fig. 4, four different stages are revealed within four different delay intervals. For the time delay equaling 0, a high value of ISI indicates the intermittent firing behavior which corresponds to Fig. 2(a). For the first stage, where the time delay equals 0–1100, the violent oscillation shows that the delay can disturb or even destroy the firing state (when no interspike interval happens, we set ISI = 0). At the second stage, delay ranges from 1100 to 2100, with the ISI oscillating slightly, and irregular zigzag patterns emerge. In this stage, the average ISI is around 1000. At the next stage, delay ranges from 2200 to 3500. Regular zigzag patterns appear with steady ISIs, and the average ISI is around 500, which is half compared with the irregular zigzag patterns, reflecting a frequency-doubling phenomenon. Recently, Lorach *et al.* [35] investigated the retinal neurons in rats experimentally. They found the frequency-doubling phenomenon and stated this phenomenon is indicative of nonlinear spatial summation. We suspected here that the nonlinear spatial summation they stated might be related to the time delay, as the similar frequency-doubling could be seen from the second to the third stage. Finally, at the last stage, firing behaviors transit from regular zigzag patterns to antiphase synchronization along with frequency increasing again. It is worth noting that there is a decrease of the ISIs between different stages, and after the decrease the ISIs increase gradually (this is also true for the interburst intervals as is seen later).

The regular zigzag pattern is not present in Ref. [18]. It is natural to ask where this phenomenon originated from. Can the randomness of the delay induce this pattern? To answer this question, the distance-dependent delay is replaced with a random delay, which reads $\tau_{ij} = \mathrm{int}(R\xi + \tau_0)$, where int$(\cdot)$ calculates the nearest integer of the quantity inside the brackets due to the discrete map. Here, τ_0 is the common delay shared by all the connected neurons and ξ is a uniformly distributed noise on the interval [0,1] which contributes to the randomness of the delay. $R = 10$ is the strength of the noise. The corresponding spatiotemporal patterns and ISIs

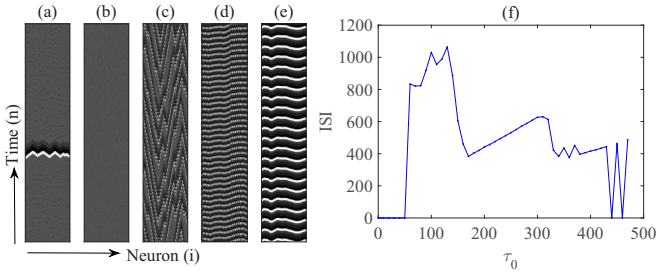

FIG. 5. Spatiotemporal patterns and ISIs of $x^i(n)$ for the random delayed neuronal network with different time delays. From (a) to (e), the common time delay τ_0 equals 0, 50, 130, 230, and 450. (f) is the ISI calculated for different delays. The color is linearly divided into ten levels with white depicting 0.0 and black depicting –1.5. Other parameters are the same as in Fig. 2.

with the increase of the delay are illustrated in Fig. 5. From Fig. 5(a) to Fig. 5(e), intermittent firing behavior, delay disturbed phenomenon, irregular zigzag pattern, antiphase synchronization, and in-phase synchronization are observed. The change of ISIs looks similar to Fig. 2 at first sight. However, there is no regular zigzag pattern between the irregular zigzag pattern and antiphase synchronization. Thus, the regular zigzag pattern is not induced by the randomness of delay. It is interesting to note that the frequency-doubling phenomenon still exists in the random delayed network [see Fig. 5(f)].

To get a deeper insight into the regular zigzag pattern, we define a distance adjusting parameter t_d. And now we can define this delay time between neurons i and j as $\tau_{ij} = \mathrm{int}\{\tau_e[(\langle d_{ij}\rangle - d_{ij})t_d + d_{ij}]\}$, where d_{ij} is the same as defined previously; $\langle d_{ij}\rangle$ is the mean of d_{ij} for all connected neurons. For $t_d = 0$, τ_{ij} is the same as in Eq. (2); for $t_d = 1$, identical delays are assumed for all coupling neurons. Thus for $t_d \in [0,1]$, the delays can range from distance dependent to identical. For two end points, ISIs are illustrated in Fig. 6(a). The two curves are qualitatively the same, but if we compare the spatiotemporal pattern at the same element delay, e.g., $\tau_e = 2400$, for identical delay ($t_d = 1$), the collective firing behavior is antiphase, while for distance-dependent delay ($t_d = 0$), it is regular zigzag pattern. And at $\tau_e = 4100$, for identical delay ($t_d = 1$), the collective firing behavior is in phase, while for distance-dependent delay ($t_d = 0$), it is antiphase. What happened when t_d increases from 0 to 1? We calculate ISIs for $t_d = 0$, 0.1, 0.2, and 0.3 as is plotted in Fig. 6(b). As t_d increases, ISIs become flatter between antiphase synchronization and regular zigzag pattern, and the inset shows the gradual overlapping of the two stages [Fig. 6(b)], finally, the two stages are totally replaced by antiphase (not shown). Above all, we have seen that the regular zigzag pattern is only present when delay is distance dependent (for small t_d). When delay becomes identical, the regular zigzag pattern will be overlapped by antiphase. A similar zigzag pattern is also studied in Ref. [24], where the pattern is induced by inhomogeneous synaptic weights or the cooperative effect of inhomogeneous delays and synaptic weights. The models in Ref. [24] are a ring of coupled limit cycle (LC) oscillators and FHN neurons coupled in a ring via excitatory chemical synapses, and both are unidirectionally

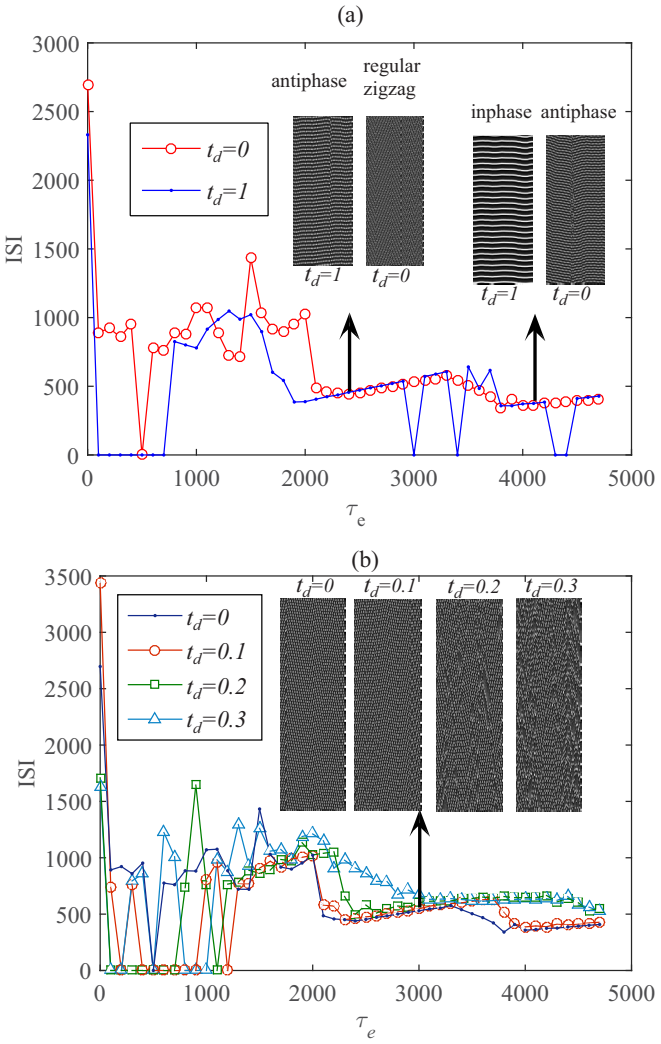

FIG. 6. ISIs of $x^i(n)$ for different distance adjusting parameter t_d with different element time delays. (a) ISI for $t_d = 0$ and $t_d = 1$. Inset: left: spatiotemporal patterns at $\tau_e = 2400$; right: spatiotemporal patterns at $\tau_e = 4100$. (b) ISI for $t_d = 0$, 0.1, 0.2, and 0.3. Inset: spatiotemporal patterns at $\tau_e = 3000$.

coupled. The main differences of our model from theirs are the coupling topology (bidirectionally, small world for ours) and the distance-dependent delay. In contrast to the detailed theoretic analysis in Ref. [24], analytical results are hopeless in our model for two reasons. First, the Gaussian noise added to the fast variable made Eq. (1) a stochastic problem. Second, the randomness of the rewiring made the topology of the network uncertain. Simplifications of the model and deeper research on the mechanism will be our future work.

Next, the generic property of these transitions, especially the regular zigzag pattern, is investigated for another value of $\alpha = 2.9$; other parameters are the same as in Fig. 2. In this case, noise is still taken into consideration for three reasons, although neurons can fire without noise. First, the purpose here is to study the genericity when neurons are under different firing states (spiking and bursting); thus changing other control parameters is unnecessary compared with the former case. Second, noise is inherent in neurons as has been clarified in the Introduction. Third, noise is preserved as a

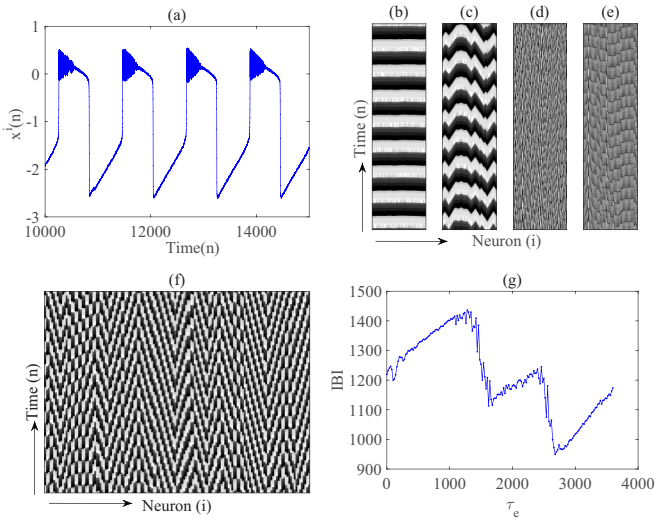

FIG. 7. Time series, spatiotemporal patterns and interburst intervals (IBIs) of $x^i(n)$. (a) Typical bursting without time delay. From (b) to (e), spatiotemporal patterns with different element time delays; τ_e equals 0, 150, 1950, and 3300 ($r = 4$). (f) is the enlargement of (d), which shows the regular zigzag pattern. The color is linearly divided into ten levels with white depicting 0.5 and black depicting –2.5. (g) is the IBI on different element time delays. Parameters: $a = 2.9$; others are the same as in Fig. 2.

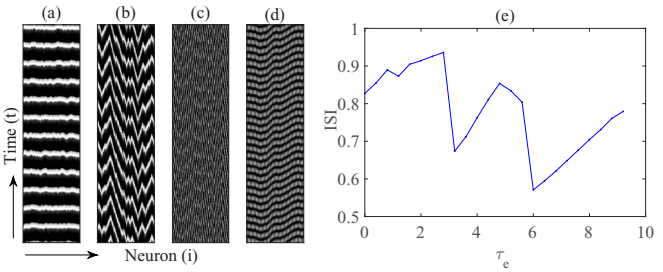

FIG. 8. Spatiotemporal patterns and ISIs of $v^i(t)$ for FHN neurons. From (a) to (d), spatiotemporal patterns (time ranges from 50 to 60 s and integral step is 0.001) with different element time delays, τ_e equals 0, 1.6, 4, and 7.2 ($r = 1$). (c) Exhibits the regular zigzag pattern. The color is linearly divided into ten levels with white depicting 1 and black depicting 0. (e) is the ISI on different element time delays. Other parameters are in the text.

perturbation, which makes the generic property more generic. The single neuron will exhibit bursting behaviors without delay as in Fig. 7(a). Figures 7(b)–7(e) are bursting synchronization, irregular zigzag pattern, regular zigzag pattern, and antiphase bursting synchronization, respectively. Interburst intervals (IBIs) are calculated in Fig. 7(g) to assist in the quantitative analysis for these transitions, whereby the increase of the frequency (in this case, the bursting frequency) can still be seen in this case.

Since the Rulkov model is a map model, in order to take a look at a more realistic neuron model, we examine the FitzHugh-Nagumo model [9], which is a simplified version of the Hodgkin-Huxley neuron model [8]. The equations are as follows:

$$\begin{aligned} c\frac{dv}{dt} &= v(v-a)(1-v) - u + I_{\text{ext}}, \\ \frac{du}{dt} &= v - u - b, \end{aligned} \tag{3}$$

where v represents a dimensionless membrane voltage and u is the slow variable compared to v. c is a time scale separation parameter, and I_{ext} is an external current. We fix $c = 0.005, a = 0.4, b = 0.2$, and $I_{\text{ext}} = 0.015$. After including delta-correlated Gaussian white noise $\xi(t)$ and small-world coupling, Eq. (3) becomes

$$\begin{aligned} c\frac{dv_i}{dt} &= v_i(v_i-a)(1-v_i) - u_i + I_{\text{ext}} + w\xi^i(t) \\ &\quad + D\sum_{j=1,2\cdots N} \varepsilon_{ij}[v_j(t-\tau_{ij}) - v_i], \\ \frac{du_i}{dt} &= v_i - u_i - b. \end{aligned} \tag{4}$$

Note that we have omitted time t in variables v and u for simplification except the delay term. We take noise intensity $w = 10^{-3}$, coupling strength $D = 0.015$, the rewiring probability $p = 0.1$, and $N = 150$. The spatiotemporal patterns and ISIs are in Fig. 8. From Figs. 8(a)–8(d), four different stages are seen, especially the third stage: regular zigzag pattern. Other stages are, in Fig. 8(a): in-phase synchronization; Fig. 8(b): irregular zigzag pattern; Fig. 8(d): antiphase synchronization. To compare the Rulkov map and FHN model more deeply, we assume they oscillate in the same frequency when they are in the same stage. Specially, in the regular zigzag stage, the ISI of FHN [Fig. 8(e)] is around 0.75 s, and the element time delay is around 4 s (note that actual delay needs to be multiplied by distance). For the Rulkov model (Fig. 4), the ISI is around 500 (unknown unit), and the element time delay is 3000 (unknown unit). Our assumption that both models have the same ISI in this stage allows estimating the unknown unit as 0.75/500 s. Thus the element time delay is around $3000\frac{0.75}{500}$ s $= 4.5$ s. We can see that the two models have similar element time delays when they are in the same stage.

Finally, in order to study the robustness of these firing behaviors and transitions related to other parameters, ISIs are computed on different values of network size, rewiring probability, noise strength, and coupling strength for the same range of time delays. The results are shown in Fig. 9. In general, changing these parameters will not qualitatively alter the transitions that we previously discussed. However, the dependence on these parameters is distinct from each other. From Figs. 9(b) and 9(c), we can see that the change of rewiring probability and noise strength makes little difference on the profile of the delay-ISI curves, while for Fig. 9(a), increasing the network size will make a right shift on the delay-ISI curves. That means under the same conditions it needs a larger time delay to produce these transitions for a larger network. Last, as is illustrated in Fig. 9(d), the coupling strength seems to have the greatest impact on our system. On one hand, a left shift can be observed as the coupling strength increases, which proves that a higher coupling strength leads to a faster transition. On the other hand, a large coupling may break down the third stage. Above all, within a proper range of the parameters, these firing behaviors and their transitions can be preserved while the robustness to these parameters may differ.

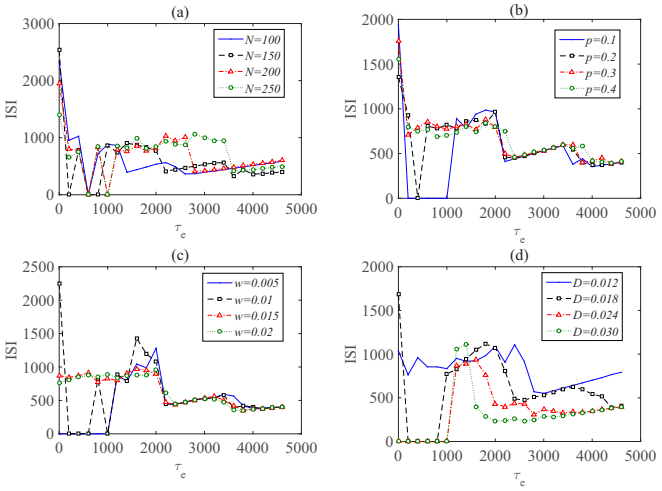

FIG. 9. The robustness of other parameters on these firing behaviors and transitions. From (a) to (d), the ISIs of $x^i(n)$ for network size, rewiring probability, noise strength, and coupling strength with different element time delays. Parameters are the same as in Fig. 2 except the parameter considered.

IV. SUMMARY AND DISCUSSION

We studied the effects of time delay related to the distance between neurons in small-world noisy networks. Each neuron was modeled by a Rulkov map with electrical synapses coupling and Gaussian noise was added to facilitate the neurons to fire frequently. Within the range of the delay researched in this paper, four stages can be identified by different firing behaviors. At first, the time delay will disturb or even destroy the firing state. Secondly, by increasing the delay, irregular zigzag patterns emerge, which are actually lag synchronizations by computing the similarity function. At the third stage, an interesting phenomenon exhibits regular zigzag pattern. Through the analysis of the interspike intervals, a frequency doubling is found compared with the former irregular zigzag patterns. At the last stage, a transition from regular zigzag patterns to antiphase synchronizations can be observed, whereby the frequency increases again. The regular zigzag pattern is proved to be induced by the distance-dependent delay by comparing with the random delay and further by introducing a distance adjusting parameter. Furthermore, the above transitions can be observed when neurons are in the bursting state, which shows these transitions are generic for different firing behaviors. Then, we extend our study to a more realistic biological model (FHN neurons), and find similar results. Finally, the robustness of these transitions to network size, rewiring probability, noise strength, and coupling strength is also demonstrated, although the individual differences of these parameters exist.

Time delay has drawn much attention and been investigated a lot in theoretical neuronal networks. However, its mechanism and complex roles in real biological neurons are still a mystery to be uncovered. In this work, the distance between neurons has been considered, which naturally stems from the finite information transmission speed. This is just an initial exploration as we take the time delay to be linearly related to the distance while the real biological neurons may have complex nonlinearity which is the next step to be investigated. We hope this work can help us better understand the firing behaviors and the transitions among them in real neuronal networks.

ACKNOWLEDGMENTS

This research was supported by the National Natural Science Foundation of China (Grants No. 11472126 and No. 11232007), the Research Fund of State Key Laboratory of Mechanics and Control of Mechanical Structures (Nanjing University of Aeronautics and Astronautics) (Grant No. 0113G01), and the Project Funded by the Priority Academic Program Development of Jiangsu Higher Education Institutions (PAPD).

[1] D. J. Watts and S. H. Strogatz, Nature **393**, 440 (1998).
[2] M. Barahona and L. M. Pecora, Phys. Rev. Lett. **89**, 054101 (2002).
[3] M. D. Humphries, K. Gurney, and T. J. Prescott, Proc. R. Soc. London, Ser. B **273**, 503 (2006).
[4] M. Perc, Chaos, Solitons Fractals **31**, 280 (2007).
[5] D. S. Bassett and E. T. Bullmore, Neuroscientist **12**, 512 (2006).
[6] L. F. Lago-Fernandez, R. Huerta, F. Corbacho, and J. A. Siguenza, Phys. Rev. Lett. **84**, 2758 (2000).
[7] Y. Zheng, Q. Wang, and M.-F. Danca, Cognitive Neurodynamics **8**, 143 (2014).
[8] A. L. Hodgkin and A. F. Huxley, J. Physiol. **117**, 500 (1952).
[9] R. FitzHugh, Biophys. J. **1**, 445 (1961).
[10] J. L. Hindmarsh and R. M. Rose, Proc. R. Soc. London, Ser. B **221**, 87 (1984).
[11] C. Morris and H. Lecar, Biophys. J. **35**, 193 (1981).
[12] N. F. Rulkov, Phys. Rev. Lett. **86**, 183 (2001).
[13] N. F. Rulkov, Phys. Rev. E **65**, 041922 (2002).
[14] C. A. S. Batista, A. M. Batista, J. A. C. de Pontes, R. L. Viana, and S. R. Lopes, Phys. Rev. E **76**, 016218 (2007).
[15] M. V. Ivanchenko, G. V. Osipov, V. D. Shalfeev, and J. Kurths, Phys. Rev. Lett. **93**, 134101 (2004).
[16] Q. Y. Wang, Q. S. Lu, and G. R. Chen, EPL **77**, 10004 (2007).
[17] Q. Y. Wang, Z. S. Duan, L. Huang, G. R. Chen, and Q. S. Lu, New J. Phys. **9**, 383 (2007).
[18] Q. Wang, Z. Duan, M. Perc, and G. Chen, EPL **83**, 50008 (2008).
[19] M. Dhamala, V. K. Jirsa, and M. Z. Ding, Phys. Rev. Lett. **92**, 074104 (2004).
[20] K. Gopalsamy and I. Leung, Physica D **89**, 395 (1996).
[21] Q. Wang, M. Perc, Z. Duan, and G. Chen, Chaos **19**, 023112 (2009).
[22] B. M. Adhikari, A. Prasad, and M. Dhamala, Chaos **21**, 023116 (2011).
[23] P. Perlikowski, S. Yanchuk, O. V. Popovych, and P. A. Tass, Phys. Rev. E **82**, 036208 (2010).

[24] S. Yanchuk, P. Perlikowski, O. V. Popovych, and P. A. Tass, Chaos **21**, 047511 (2011).
[25] S. Lakshmanan, K. Mathiyalagan, J. H. Park, R. Sakthivel, and F. A. Rihan, Neurocomputing **129**, 392 (2014).
[26] M. S. Ali, S. Arik, and R. Saravanakurnar, Neurocomputing **158**, 167 (2015).
[27] Z. Feng and J. Lam, IEEE Trans. Neural Networks **22**, 976 (2011).
[28] G. Tang, K. Xu, and L. Jiang, Phys. Rev. E **84**, 046207 (2011).
[29] K. Trojanowski and L. Longa, Acta Phys. Pol., B **44**, 991 (2013).
[30] S. O. Jeong, T. W. Ko, and H. T. Moon, Phys. Rev. Lett. **89**, 154104 (2002).
[31] T.W. Ko and G. B. Ermentrout, Phys. Rev. E **76**, 056206 (2007).
[32] B. Ermentrout and T.W. Ko, Philos. Trans. R. Soc., A **367**, 1097 (2009).
[33] B. Lindner, J. García-Ojalvo, A. Neiman, and L. Schimansky-Geier, Phys. Rep. **392**, 321 (2004).
[34] M. G. Rosenblum, A. S. Pikovsky, and J. Kurths, Phys. Rev. Lett. **78**, 4193 (1997).
[35] H. Lorach, G. Goetz, R. Smith, X. Lei, Y. Mandel, T. Kamins, K. Mathieson, P. Huie, J. Harris, A. Sher, and D. Palanker, Nat. Med. **21**, 476 (2015).